Dalton Transactions

PAPER

View Article Online
View Journal | View Issue

Cite this: *Dalton Trans.*, 2014, **43**, 14701

Discriminate sensing of pyrophosphate using a new tripodal tetramine-based dinuclear Zn(II) complex under an indicator displacement assay approach†

Sarayut Watchasit,[a] Pattira Suktanarak,[b] Chomchai Suksai,*[b] Vithaya Ruangpornvisuti[a] and Thawatchai Tuntulani*[a]

Received 30th August 2013,
Accepted 29th July 2014

DOI: 10.1039/c3dt52392f

www.rsc.org/dalton

In this research, the dinuclear Zn(II) complex of anthracene based tripodal tetramine Zn_2L was synthesized, and its sensing abilities towards anions was investigated using the indicator displacement assay (IDA) approach with four complexometric indicators: pyrocatechol violet (PV), bromopyrogallol red (BPG), methylthymol blue (MTB) and xylenol orange (XO). UV-vis spectrophotometry results indicated that the Zn_2L–MTB ensemble sensor could discriminate the pyrophosphate anion (PPi) from other phosphate containing anions. ^1H and ^{31}P NMR spectroscopy as well as DFT calculations confirmed that PPi bound to Zn_2L in a 2 : 2 manner. Both NMR spectroscopy and UV-vis spectrophotometry suggested that the two bulky tripodal tetramine units in Zn_2L played an important role to provide the ensemble cleft for MTB, giving rise to an ensemble that could be displaced exclusively by PPi. The detection limit of PPi for the reported IDA system was 0.3 μM in 20% (v/v) water–acetonitrile buffered at pH 7.4 with HEPES.

1. Introduction

Recently, artificial receptors for recognition and sensing of phosphate anions have attracted chemists' attention due to their importance in living systems.[1] Great attention has been given to the design of chemical sensors for the pyrophosphate anion, $P_2O_7^{4-}$ or PPi.[2] Such an interest stems from the fact that PPi plays an important role in many biological processes. In particular, PPi participates in ATP hydrolysis and is involved in DNA or RNA polymerase reactions.[3] Moreover, the amount of PPi has recently been monitored in patients with calcium pyrophosphate dihydrate (CCPD) crystal deposition disease (also known as chondrocalcinosis), as the disease has been shown to cause high synovial fluid PPi levels in patients.[4] Therefore, discriminate sensing of PPi under physiological conditions remains a significant challenge.

The indicator displacement assay (IDA) is the most simple, convenient and increasingly popular approach for naked-eye sensing of anions.[5] Recently, Zn(II)–dipicolyl amine (DPA) complexes have been employed in anion recognition and sensing of phosphate species.[6] However, most of the IDA systems using dinuclear Zn(II)–DPA complexes show low selectivity toward PPi[7] or encounter interference from other phosphate species such as PO_4^{3-} (Pi) and adenosine triphosphate (ATP).[8] A few IDA receptors for discriminate sensing of PPi using dinuclear Zn(II)–DPA complexes have been reported.[9] Jolliffe and coworkers have synthesized a library of anion receptors comprising linear[9a] and cyclic[9b] peptide scaffolds bearing dinuclear Zn(II)–DPA units which could be located at different positions on the cyclic peptide. The ensemble cleft of the cyclic peptide receptors and indicators could be varied, and the discrimination between PPi and other phosphate containing anions by the IDA approach was achieved.

Although the sensing ability of chemosensing ensembles formed by the flexible scaffold could be easily tuned by appropriate indicators and may provide effective discrimination of PPi from other anions, the coordination chemistry of the dinuclear Zn(II) could play an important role in selective sensing as well. Recently, Lippard and colleagues have shown that a tripodal tetramine unit on the fluorescein scaffold can be used successfully as a neuronal Zn^{2+} sensor and gives a better sensing property than the precursor one containing DPA binding units.[10] We have prepared an IDA receptor for PPi

[a]*Department of Chemistry, Faculty of Science, Chulalongkorn University, Bangkok 10330, Thailand. E-mail: tthawatc@chula.ac.th; Fax: +66 2 2187598; Tel: +66 2 2187643*

[b]*Department of Chemistry and Center for Innovation in Chemistry, Faculty of Science, Burapha University, Chonburi 20131, Thailand. E-mail: jomjai@buu.ac.th; Fax: +66 038 393494; Tel: +66 038 103111*

†Electronic supplementary information (ESI) available: Synthetic scheme of Zn_2L, ^1H and ^{13}C NMR spectra of L and Zn_2L, ^1H and ^{31}P NMR spectra of the Zn_2L–MTB ensembles and replacement with PPi and UV-vis spectra of Zn_2L with various indicators. See DOI: 10.1039/c3dt52392f

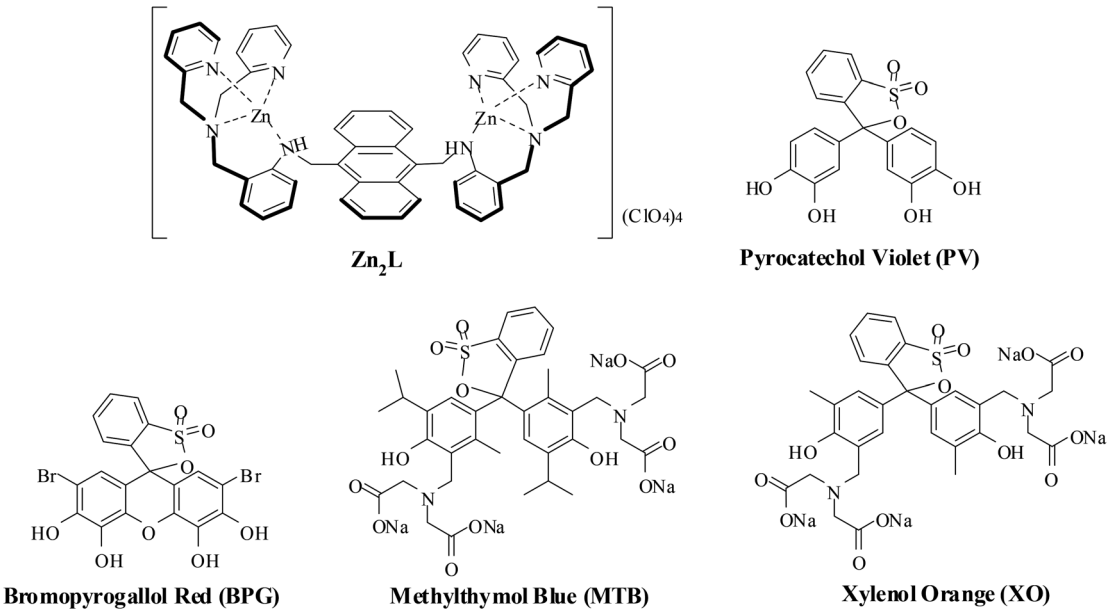

Chart 1 Structures of Zn_2L and indicators employed in the IDA studies.

from the dinuclear Cu(II) complexes of di-tripodal tetramine units on the calix[4]arene scaffold.[11] In this paper, we synthesize a new ligand (L) containing two tripodal tetramine units linked to the anthracene scaffold and its dinuclear Zn(II) complex (Zn_2L). We explore the binding properties of Zn_2L with PPi and an indicator by using ^1H and ^{31}P NMR spectroscopy. The structure of the complex between Zn_2L and PPi is calculated using DFT. The selective sensing ability of Zn_2L toward PPi in aqueous solution using the IDA approach is established using UV-vis spectrophotometry and possible species in the aqueous solution are analyzed from the UV-vis spectra using the SPECFIT32 program.[12] The structures of Zn_2L and various commercially available indicators employed in this study are presented in Chart 1.

2. Experimental

2.1 General method

All chemicals were of analytical grade and used without further purification. Sterile water for injection was obtained from General Hospital Products Public Co., Ltd. (Pathum Thani, Thailand). Zn_2L and indicator solutions were freshly prepared[10,13] just before the NMR and UV-vis experiments. ^1H-, ^{13}C- and ^{31}P-NMR were carried out using the Bruker AVANCE 400 MHz Ultra Shield spectrometer. All UV-vis absorption spectra were recorded using an Agilent 8453 UV-vis spectrophotometer. Tripodal tetramine (**a**) was synthesized according to the procedure reported previously.[10,13]

2.2 Synthesis of L

A mixture of tripodal tetramine (**a**) (1.93 g, 6.34 mmol) and 9,10-diformylanthracene (**b**) (0.64 g, 2.73 mmol) was dissolved in dry CH_3CN (50 mL) (Scheme S1 in the ESI†). The reaction mixture was refluxed under nitrogen for 12 h. After the solvent was removed, the product was obtained as a dark solid (quantitative yield). The crude imine was dissolved in MeOH (100 mL) and the solution was cooled to −5 °C. Subsequently, $NaBH_4$ (4.18 g, 110 mmol) was added to the brown solution, and the mixture was refluxed for 12 h under a nitrogen atmosphere. After the mixture cooled to room temperature, water (150 mL) was added and the mixture was evaporated to remove MeOH. The residue was dissolved in CH_2Cl_2 (150 mL) and the organic layer was washed with water (3 × 100 mL), dried with anhydrous $MgSO_4$, and the solvent was removed. The light yellow solid of ligand L was obtained after recrystallization of the crude product in MeOH (0.90 g, 41%). ^1H-NMR (400 MHz, $CDCl_3$, ppm): δ 8.45 (q, J = 3.6 Hz, 4H, Ar*H*), 8.03 (d, J = 4.4 Hz, 4H, Ar*H*), 7.58 (q, J = 3.6 Hz, 4H, Ar*H*), 7.38 (t, J = 8 Hz, 2H, Ar*H*), 7.18 (d, J = 7.2 Hz, 2H, Ar*H*), 7.10 (d, J = 8 Hz, 2H, Ar*H*), 6.73 (m, 10H, Ar*H*), 6.51 (d, J = 7.6 Hz, 4H, Ar*H*), 6.33 (s, 2H, –N*H*–), 5.28 (s, 4H, –CH_2–), 3.59 (s, 4H, –CH_2–), 3.52 (s, 8H, –CH_2–). ^{13}C-NMR (100 MHz, $CDCl_3$, ppm): δ 158.43, 148.58, 148.05, 135.79, 131.43, 131.01, 130.89, 129.00, 126.13, 125.51, 122.55, 122.24, 121.96, 121.44, 116.69, 109.63, 60.35, 58.50, 40.96. ESI-MS (positive mode); 811.4281 $[M + H]^+$. Elemental analysis calculated for $C_{54}H_{50}N_8$: C, 79.97; H, 6.21; N, 13.82; found C, 79.89; H, 6.16; N, 13.87.

2.3 Synthesis of Zn_2L

The ethanolic solution of $Zn(ClO_4)_2{\cdot}6H_2O$ (37.2 mg, 0.1 mmol) was added to the ethanolic suspension of L (24.3 mg, 0.03 mmol) (Scheme S1 in the ESI†), the color of the solution changed to yellow immediately. Then, the yellow solution was refluxed under nitrogen for 12 h. After cooling to room temperature, the yellow solids precipitated, and were filtered and washed with CH_2Cl_2 and MeOH to obtain Zn_2L (35.4 mg,

88%). ^{1}H-NMR (400 MHz, 20% (v/v) D_2O–CD_3CN, ppm): δ 8.70 (bs, 4H, Ar*H*), 7.87 (bm, 8H, Ar*H*), 7.48 (bm, 4H, Ar*H*), 7.34 (bs, 8H, Ar*H*), 7.20 (d, J = 7.6 Hz, 2H, Ar*H*–NH–), 6.75 (t, J = 7.6 Hz, 2H, Ar*H*–NH–), 6.25 (t, J = 7.6 Hz, 2H, Ar*H*–NH–), 5.27 (bd, J = 7.6 Hz, 2H, Ar*H*–NH–) 4.98 (bs, 4H, Ar–NH–C*H*$_2$–), 4.29 (m, 12H, Ar–C*H*$_2$–). ^{13}C-NMR (100 MHz, 20% (v/v) D_2O–CD_3CN, ppm): δ 154.76, 147.63, 141.88, 140.97, 133.37, 129.79, 129.09, 128.72, 127.15, 126.23, 125.80, 124.93, 124.56, 124.34, 124.00, 59.02, 27.84, 45.11. ESI-MS (positive mode); 1235.0554 $[M + 3ClO_4^-]^+$. Elemental analysis calculated for $C_{54}H_{50}Cl_4N_8O_{16}Zn_2{\cdot}H_2O{\cdot}CH_2Cl_2$: C, 45.79; H, 3.77; N, 7.77; found C, 45.66; H, 3.76; N, 7.93. **Caution**: perchlorate salts are potentially hazardous and should be handled with care!

2.4 Screening tests of indicators for selective PPi sensing

For the colorimetric detection of PPi, a solution of each indicator, 400 μM (0.2 mL) in 20% (v/v) water–acetonitrile solution buffered at pH 7.4 with HEPES, was added into a solution of Zn_2L 20 μM (2 mL) in the same solvent system. Subsequently, 0.3 mL of the tetrabutylammonium salt of the anion (1 mM) was then added to the as-prepared ensemble. The resulting mixtures were allowed to stand still for 5 min and then subjected to UV-vis spectroscopic measurements. Photographs were taken using a digital camera (Canon EOS Kiss X5, Japan).

2.5 UV-vis titrations under the indicator displacement assay

All spectrometric titrations were performed in 20% (v/v) water–acetonitrile solutions buffered at pH 7.4 with HEPES (10 mM) in quartz cuvettes. Ensemble formation constants were determined by adding aliquots of 400 μM (10 μL) complex solution to 20 μM (2 mL) of each indicator using a syringe. After each addition, the absorption spectra of the indicator solution were recorded. Similar titration experiments were performed with PPi. In a typical titration, aliquots of the solution of PPi 400 μM (10 μL) were added to 20 μM (2 mL) of 1 : 1 or 1 : 2 ensemble solution of Zn_2L–MTB. The ensemble formation constants and the apparent competitive binding constants were calculated using the SPECFIT32 program.[12]

2.6 NMR titration experiment

Generally, all reagents in the NMR titration experiments were prepared in 20% (v/v) D_2O–CD_3CN. For PPi titration, aliquots of PPi 0.05 M (5 μL) were added to the 0.5 mL solution of Zn_2L (5 mM) using a syringe. For MTB titration, aliquots of MTB 0.05 M (5 μL) were added to the 0.5 mL solution of Zn_2L (5 mM) using a syringe. For MTB displacement titrations, aliquots of PPi 0.05 M were added to the 0.5 mL solution of 1 : 1 and 1 : 2 ensemble (5 mM) solutions of Zn_2L–MTB. Subsequently, ^{1}H or ^{31}P NMR spectra were recorded.

3. Results and discussion

3.1 Synthesis of L and Zn_2L

Ligand L was straightforwardly synthesized in a moderate yield (41%) by a Schiff base condensation between tripodal tetramine (**a**) and 9,10-diformylanthracene (**b**) in refluxing acetonitrile followed by *in situ* reduction using $NaBH_4$ in refluxing methanol (Scheme S1 in the ESI†). The dinuclear zinc(II) complex, Zn_2L, was readily obtained by refluxing $Zn(ClO_4)_2{\cdot}6H_2O$ with L in ethanol in 88% yield. Ligand L and the Zn_2L complex were characterized by standard analytical methods (Fig. S1–S5 in the ESI†). The ^{1}H NMR spectrum of Zn_2L in 20% D_2O–CD_3CN showed rather broad signals, compared to that of the free ligand. A multiplet signal of methylene protons of the two pyridine groups and the amine group appeared at 4.29 ppm. The aromatic protons of the aryl rings connecting to the amine group appeared at more upfield positions compared to that of L, probably due to the coordination of the N atom to the Zn(II) center. We proposed that L behaved as a tetradentate ligand to coordinate Zn(II) using 4 N atoms of the tripodal tetramine unit.[10]

3.2 Screening tests of indicators for selective PPi sensing

We first tested the anion sensing capabilities of the receptor Zn_2L by using an indicator displacement assay. In this study, 4 commercial dyes, pyrocatechol violet (PV), bromopyrogallol red (BPG), methylthymol blue (MTB) and xylenol orange (XO), which were complexometric indicators for the determination of metal ions were employed.[14] We prepared both 1 : 1 and 1 : 2 receptor to indicator ratios in 20% (v/v) water–acetonitrile solution buffered at pH 7.4 with HEPES to screen the sensing abilities toward PPi over other anions.

After the addition of various anions (7.5 equivalents of tetrabutylammonium salts) to four ensemble solutions, we found that only the MTB based ensemble of Zn_2L was able to discriminate PPi from other anions as indicated by a color change from blue to purple, shown in Fig. 1c. However, the PV– and BPG–Zn_2L ensembles responded to all phosphate containing anions because the color of the corresponding ensembles was converted to the color of the unbound indicators. In the case of the XO–Zn_2L ensemble, there were no significant changes upon addition of all anions. Therefore, the anions were not able to dislodge the XO indicator. Both MTB and XO have a similar core structure, they differ only in the bulky substituents on the rings. We expect that the binding affinity of the Zn_2L–indicator ensemble must play an important role in the displacement of the indicator by an anion. Compared to dinuclear Zn(II)–DPA receptors which could undergo IDA using the indicator PV,[6,15] our Zn_2L needed a different indicator due to the change in coordination chemistry around the Zn(II) center. Therefore, the binding properties of Zn_2L with PPi and the 4 indicators were studied by ^{1}H and ^{31}P NMR spectroscopy as well as UV-vis spectrophotometry.

3.3 Binding studies of Zn_2L with PPi by ^{1}H and ^{31}P NMR spectroscopy

Upon adding portions of PPi (in 20% D_2O–CD_3CN) to the solution of Zn_2L, the ^{1}H NMR spectrum of the Zn_2L starts broaden indicating a fluxional behaviour (Fig. 2). When 2 equiv. of PPi is added, the spectrum becomes resolved. All protons can be assigned by the HMQC technique. Interestingly, in the

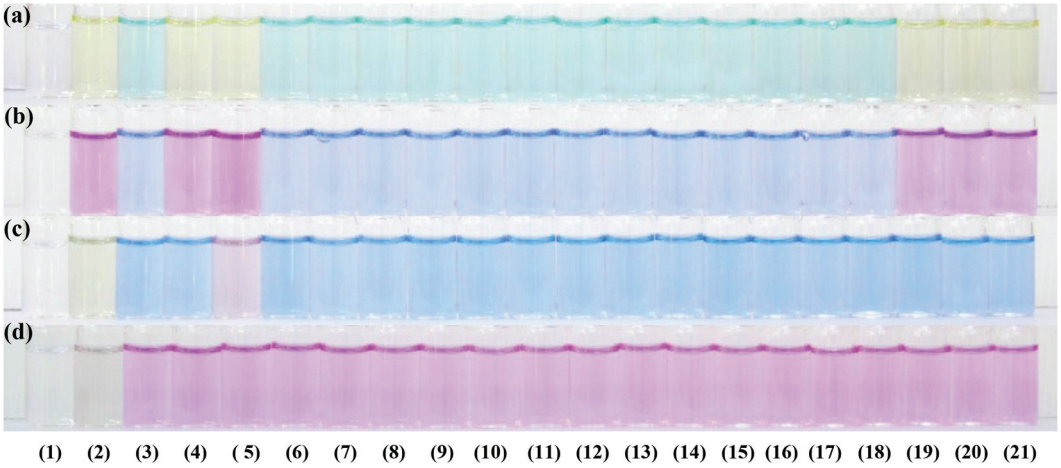

Fig. 1 Color changes of the Zn_2L-based (20 μM, 2 mL) ensembles with various indicators (400 μM, 0.2 mL) at a 1 : 2 receptor to indicator ratio (a) PV, (b) BPG, (c) MTB and (d) XO in the presence of various anions (1 mM, 0.3 mL), where (1) = Zn_2L, (2) = indicator, (3) = ensemble, (4) = HPO_4^{2-}, (5) = PPi, (6) = SO_4^{2-}, (7) = NO_3^-, (8) = CO_3^{2-}, (9) = HCO_3^{2-}, (10) = AcO^-, (11) = BzO^-, (12) = CN^-, (13) = SCN^-, (14) = OH^-, (15) = I^-, (16) = Br^-, (17) = Cl^-, (18) = F^-, (19) = AMP. (20) = ADP and (21) = ATP, respectively in 20% (v/v) H_2O–CH_3CN buffered at pH 7.4 with HEPES.

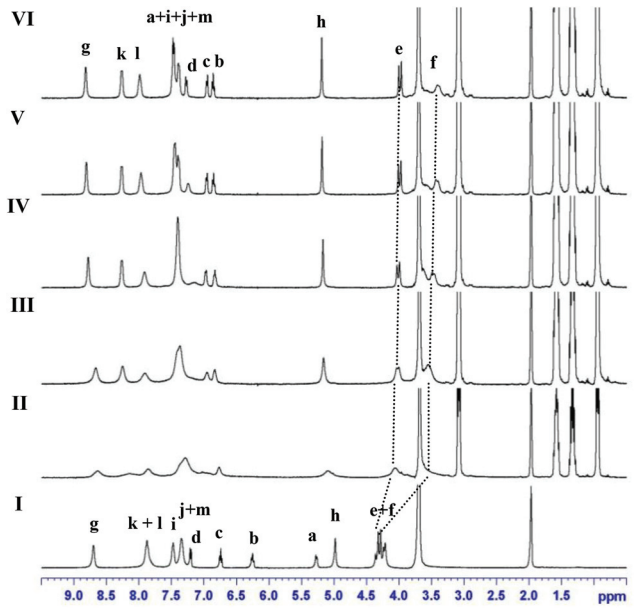

Fig. 2 ^1H NMR spectra of (I) free Zn_2L, (II) Zn_2L + PPi 0.5 equiv., (III) Zn_2L + PPi 1.0 equiv., (IV) Zn_2L + PPi 1.5 equiv., (V) Zn_2L + PPi 2.0 equiv. and (VI) Zn_2L + PPi 2.5 equiv. in 20% (v/v) D_2O–CD_3CN.

absence of PPi the aromatic proton a of the dinuclear complex Zn_2L is present in a higher magnetic field region, at δ = 5.3 ppm, probably due to the shielding effect of the ring current of the aromatic anthracene ring. Upon addition of PPi, the proton a disappears from the NMR spectrum and reappears in a more downfield region. The aromatic protons b and c move downfield and the methylene protons e and f move upfield. Therefore, protons on the aromatic ring A generally move significantly while protons g, i, j and k on the aromatic ring B move to a lesser extent. The proton h of the methylene linkage between anthracene and the tripodal tetramine unit, functioning as a pivot of the movement, stays sharp upon addition of PPi. The results imply that the aromatic ring A probably moves away from the anthracene moiety upon the binding of PPi to the Zn(II) center.

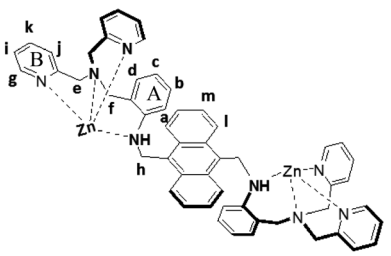

^{31}P NMR titrations of Zn_2L in 20% D_2O–CH_3CN with portions of PPi were carried out and the spectra are shown in Fig. 3. The free PPi has a signal at −6.0 ppm. It can be clearly seen that adding up to 1.0 equiv. of PPi to the solution of Zn_2L gave a single broad peak at −3.0 ppm due to the formation of a complex between an equivalent amount of Zn_2L and PPi, concomitant with the disappearance of the signal at −6.0 ppm. The single peak at −3.00 ppm implied that the two P atoms in Zn_2L-bound PPi are magnetically equivalent. Upon adding more than 1 equiv. of PPi, a signal at a more upfield position appears in the spectrum. After the addition of 4 equiv. of PPi, this peak shifts to a more downfield position, close to that of the signal of free PPi, and the signal at −3.0 ppm becomes more resolved.

The best way to obtain the exact structure of the Zn_2L–PPi complex is from the crystal structure determination. However, we cannot obtain a suitable crystal of the complex for X-ray crystallography, probably due to the mixed solvent system (H_2O–CH_3CN) used in the preparation of the complex. Based on the several binding modes of PPi toward the metal center reported previously,[16] the density functional theory (DFT) calculations of a possible complex of Zn_2L and PPi in 1 : 1 and 2 : 2 fashions were carried out to find the most stable structure

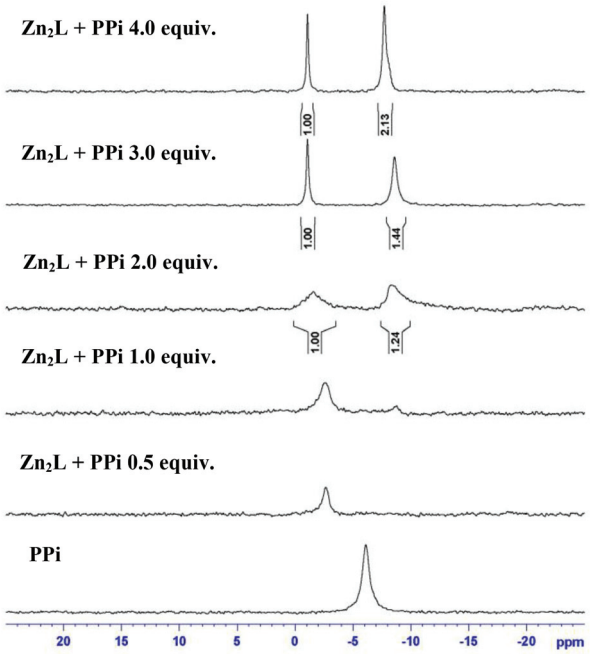

Fig. 3 ^{31}P NMR spectra of Zn_2L (5 mM) upon addition of various concentrations of PPi (0.05 M) in 20% (v/v) D_2O–CD_3CN.

instead. According to computer simulations, the 1 : 1 complex model was not possible due to too much strain in the molecule of the 1 : 1 PPi-bound Zn_2L complex. However, six conformers of dimeric 2 : 2 species represented as $2Zn_2L{\cdot}2PPi$ were found and their energies were calculated (Table S1 and Fig. S6–S11 in the ESI†). All optimized structures were obtained by DFT calculations using the B3LYP/LANL2DZ level of theory[17–19] performed with the GAUSSIAN09 program.[20] The most stable structure of $2Zn_2L{\cdot}2PPi$ is shown in Fig. 4. The dimeric species is composed of two Zn_2L and two PPi units forming a tetranuclear Zn(II) complex with PPi as bridging ligands. Two oxygen atoms on each phosphorus of PPi coordinated to one Zn^{2+} ion, the same as the structure reported by Hong *et al.*[8b] Interestingly, the calculated structure showed a high symmetry structure of the PPi units. This agreed with the result from the ^{31}P NMR spectroscopy where the two phosphorous atoms in PPi appeared as a singlet peak the in ^{31}P-NMR spectrum. In addition, the calculated structure is also relevant to the signals that appeared in the ^{1}H NMR spectrum shown in Fig. 2. The calculated dimeric structure is similar to the structure of the PPi bound-dinuclear Zn(II) complex reported by Lee *et al.*[21]

3.4 Binding studies of Zn_2L with MTB and displacement studies with PPi using ^{1}H NMR spectroscopy

Upon addition of portions of MTB (in 20% D_2O–CD_3CN) to the solution of Zn_2L (in 20% D_2O–CD_3CN), ^{1}H NMR spectra were obtained and are shown in Fig. 5. The ^{1}H NMR spectrum of Zn_2L starts to broaden after adding portions of MTB and is too complicated to assign each proton signal. However, it can be clearly seen that upon adding more than 1 equiv. of MTB to Zn_2L, the peak due to free MTB emerges in the spectrum.

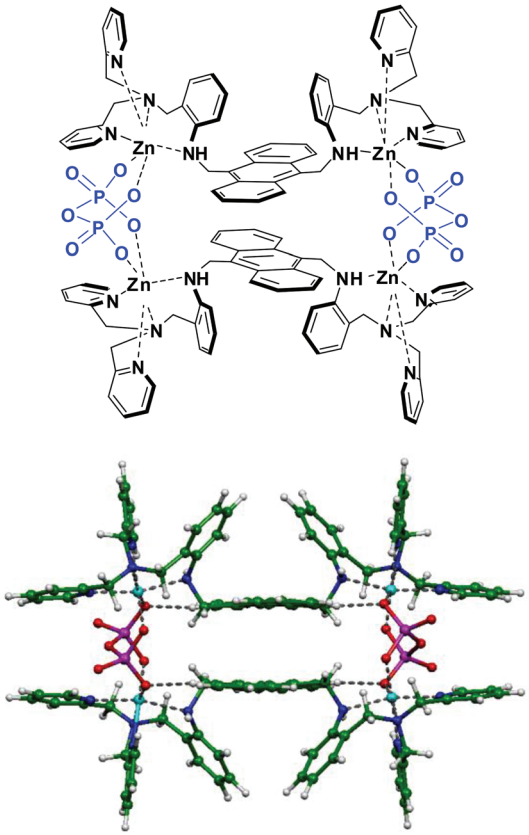

Fig. 4 The most stable DFT-calculated structure of the dimeric 2 : 2 species, $2Zn_2L{\cdot}2PPi$ complex.

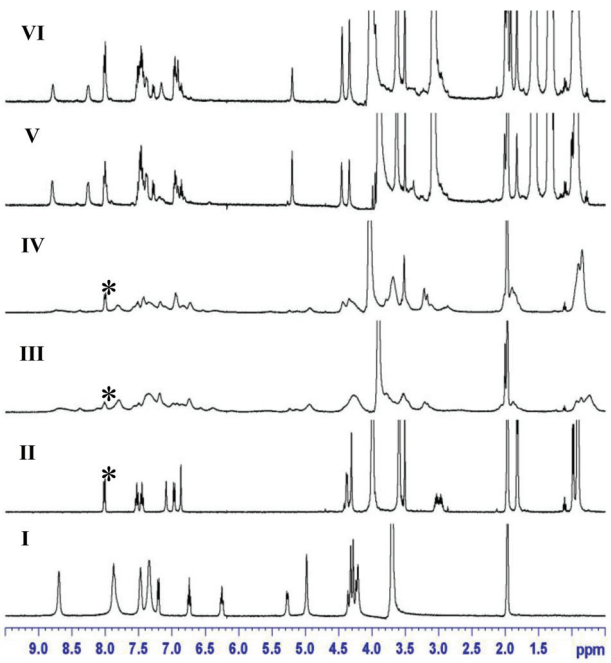

Fig. 5 ^{1}H NMR titration spectra of (I) Zn_2L (5 mM), (II) MTB, (III) $Zn_2L{\cdot}MTB$, (IV) $Zn_2L{\cdot}2MTB$, (V) $Zn_2L{\cdot}MTB$ + 2.0 equiv. of PPi and (VI) $Zn_2L{\cdot}2MTB$ + 2.0 equiv. of PPi in 20% (v/v) D_2O–CD_3CN, where * is the residue of free MTB present in the ensemble.

Therefore, ^{1}H NMR titrations of 1 : 1 and 1 : 2 ensembles of Zn_2L and MTB with PPi were carried out in 20% D_2O–CD_3CN (Fig. S12 and S13 in the ESI†). The spectra were too complicated to clearly assign the signal to particular protons. Interestingly, after more than 1 equiv. of PPi was added, the spectra of both 1 : 1 and 1 : 2 ensembles became very similar and were almost the same as those observed for the 1 : 1 species of Zn_2L·PPi shown in Fig. 2. ^{31}P NMR titrations of the 1 : 1 and 1 : 2 ensembles of Zn_2L and MTB with PPi in 20% D_2O–CD_3CN (Fig. S14 and S15 in the ESI†) gave almost identical spectra to the results shown in Fig. 3. These results confirm that MTB can be replaced by PPi, and most of the final species are PPi-bound Zn_2L.

3.5 Studies of Zn_2L–indicator ensembles by UV-vis spectrophotometry

From the above results, we can clearly see that the new Zn_2L complex can be used to detect PPi selectively. Therefore, we studied the binding behaviors in aqueous solution using UV-vis spectrophotometry. To understand the sensing phenomenon of our ensembles, we had to determine the ensemble formation constants ($\log\beta$) by employing the SPECFIT32 program. Typically, an experiment was carried out by the titration of Zn_2L to a solution of each indicator. The addition of 0–0.4 equiv. of Zn_2L to a solution of MTB, resulted in a bathochromic shift of the absorption at 450 nm to 530 nm (Fig. 6a)

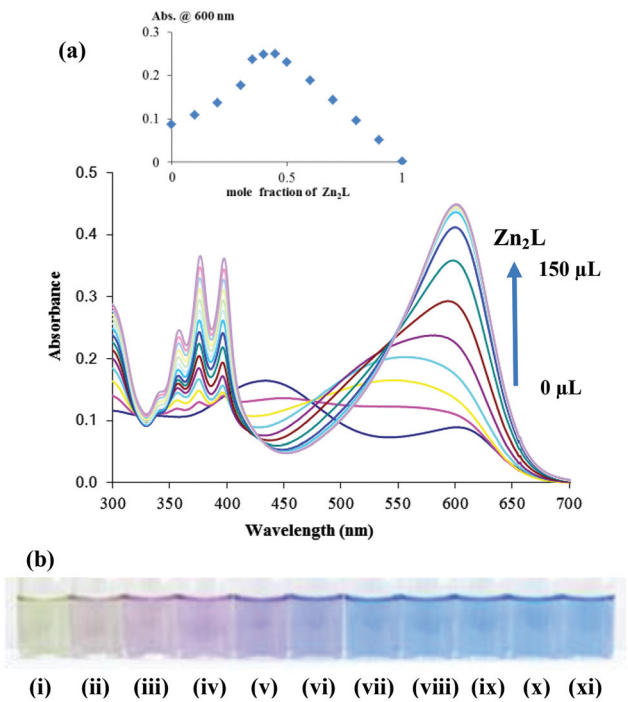

Fig. 6 (a) UV-vis spectra obtained by the addition of Zn_2L (400 µM) to a solution of MTB (20 µM), inset: Job's plot analysis of the MTB-based ensemble and (b) color changes upon increasing the amount of Zn_2L (400 µM) to the MTB (20 µM) solution: (i) free MTB, (ii) 0.1 eq., (iii) 0.2 eq., (iv) 0.3 eq., (v) 0.4 eq., (vi) 0.5 eq., (vii) 0.6 eq., (viii) 0.7 eq., (ix) 0.8 eq., (x) 0.9 eq. and (xi) 1.0 eq.

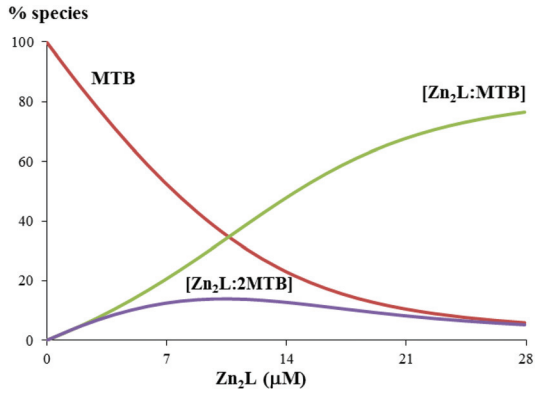

Fig. 7 Concentration profiles of the species present at equilibrium in the UV-vis titration of MTB-base ensemble, where % is referred to the total concentration of MTB.

and the color changed from pale green to violet (Fig. 6b, vials no. i–v), visible to the naked eye. Subsequently, increasing the amount of Zn_2L to the ensemble solutions, caused the bathochromic shift of the absorption at 530 nm to 600 nm and finally the blue color was observed (Fig. 6b, vials no. vi–xi). The UV-vis spectrum at 600 nm was completely saturated around 1.3 equivalents of Zn_2L. The results showed that two species were formed during the titration. From the concentration profile, upon addition of Zn_2L to the MTB solution, a complex of 1 : 2 species of Zn_2L·2MTB was present in a maximum abundance of 15% at 10 µM of Zn_2L. On further addition of Zn_2L, a 1 : 1 species of Zn_2L·MTB could form in 80% abundance, which was much higher than that of the Zn_2L·2MTB species, Fig. 7. The presence of two co-existing ensemble species (1 : 1 and 1 : 2) agreed well with the Job's plot analysis of the ensembles (Fig. 6a inset) and the unresolved ^{1}H NMR spectra shown in Fig. 5.

Ensembles of Zn_2L and PV, BPG as well as XO were also studied by UV-vis spectrophotometry, and their absorption spectra are shown in Fig. S16–S18 in the ESI.† Stepwise formation constants of all ensembles calculated by SPECFIT32 are tabulated in Table 1. The results showed that two species were formed during the titration. Upon addition of Zn_2L to the indicator (I) solution, the 1 : 2 Zn_2L·2I species occurred because the concentration of I was much higher than that of Zn_2L at the beginning of titration. Further addition of Zn_2L would yield the Zn_2L·I species. Therefore, the Zn_2L·I would exist in high concentration at the end of titrations. The presence of two co-existing ensemble species of those three indicators (1 : 1 and 1 : 2) agreed well with the Job's plots (Fig. S16–S18 in the ESI†).

Table 1 Stepwise ensemble formation constants ($\log\beta$) between Zn_2L and the indicators

	$\log\beta_1$	$\log\beta_2$
PV	3.98 ± 0.38	8.43 ± 0.22
BPG	4.76 ± 0.26	9.14 ± 0.26
MTB	6.05 ± 0.16	10.80 ± 0.32
XO	7.72 ± 0.18	13.48 ± 0.28

XO showed the highest binding constant ($\log\beta_1$) to the Zn_2L receptor compared to PV, BPG and MTB suggesting that XO could sit in the ensemble cleft with the strongest interactions with Zn_2L. The $\log\beta_1$ of MTB to Zn_2L was lower than that of XO. Presumably, the two bulky isopropyl groups of MTB, giving the more steric hindrance than XO, decreased the binding affinity of MTB to the Zn^{2+} metal ions. For PV and BPG indicators, $\log\beta_1$ values were smaller than that of XO and MTB suggesting that their structural scaffolds were less suitable for coordinating to the two metal centers in Zn_2L.

3.6 PPi sensing studies under the IDA approach

The screen test of our IDA system suggests that MTB was the best indicator to be replaced solely by PPi. In addition, results from the NMR and UV studies suggest that upon the addition of excess MTB to Zn_2L, both 1 : 1 and 1 : 2 Zn_2L–MTB were formed with the former most dominant in solution. To investigate the sensing ability of PPi under IDA experiments, the chemosensing ensembles were prepared by mixing Zn_2L and the MTB indicator in a 1 : 2 molar ratio in 20% (v/v) water–acetonitrile solution buffered at pH 7.4 with HEPES. The displacement of indicators by anions was carried out by the addition of various anions to those ensemble solutions. Subsequently, colorimetric changes as well as the UV-visible spectra changes were examined. Upon addition of various anions (as tetrabutylammonium salts, 7.5 equivalents) to the MTB–Zn_2L based ensemble solutions, only PPi could turn the color from blue to violet, while other anions did not give rise to either changes in the UV-vis spectra or in color. These results suggest that those anions did not interfere with the PPi sensing. Indeed, the lack of interference may be due to the fact that the binding affinities of the other anions with Zn_2L are weaker than that of MTB with Zn_2L. The results suggested that MTB possessed an appropriate affinity to Zn_2L to facilitate such a selective response to PPi.

The addition of PPi 0–3 equiv. to the 1 : 2 base ensemble of Zn_2L–2MTB led to the hypsochromic shift corresponding to the disappearance of the absorption band of the ensemble at 600 nm and the appearance of a new absorption band around 530 nm. The UV-vis spectrum at 530 nm was completely saturated at 3 equiv. of PPi (Fig. 8a). In addition, the color of the ensemble turned from blue to violet. The apparent competitive binding constants of PPi with Zn_2L·MTB in the displacement assay were determined by SPECFIT32 to be $\log\beta_1$ = 8.97 ± 0.28 and $\log\beta_2$ = 10.79 ± 0.28 corresponding to [Zn_2L·2PPi] and [2Zn_2L·2PPi], respectively (Fig. 8b). The presence of the [2Zn_2L·2PPi] species at the end of titration agreed well with the most stable structure shown in Fig. 4 obtained from DFT calculations. It should be noted that, the observed violet color in the PPi competition experiments was similar to the color observed in the ensemble formation experiments (see Fig. 6b, vial no. iii).

3.7 Studies of interferences and limit of detection

To further explore the effective applications of the Zn_2L–MTB ensemble, the competition experiments were also measured.

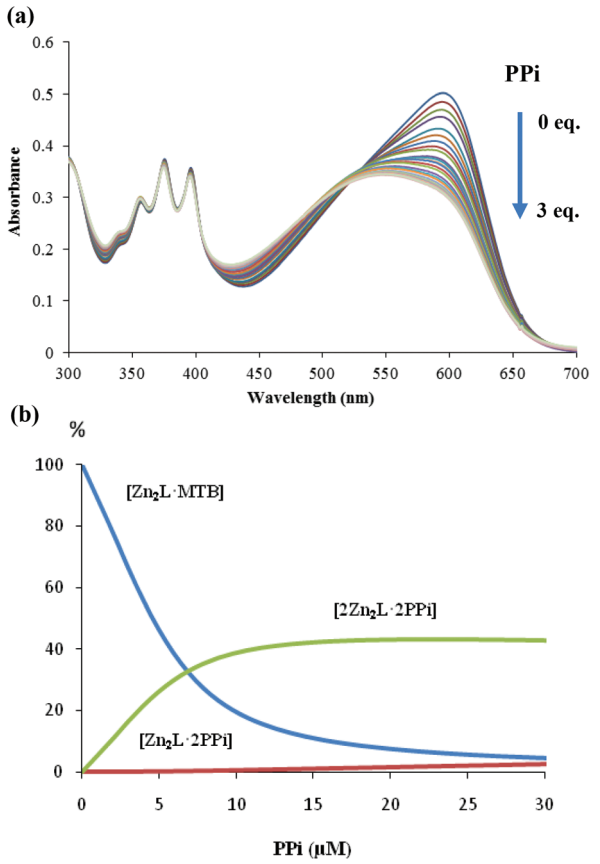

Fig. 8 (a) UV-vis spectra obtained for the addition of PPi (1 mM) to a 1 : 2 ensemble solution of Zn_2L and MTB (20 μM) and (b) concentration profiles of the species present at equilibrium in the UV-vis titration of PPi displaced [Zn_2L·MTB] ensemble.

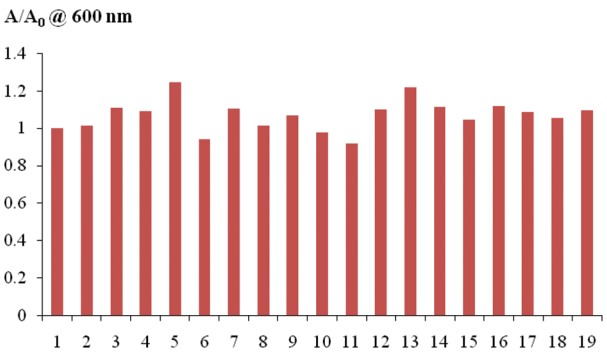

Fig. 9 Sensing of PPi in the presence of competitive anions (7.5 equivalents) in 20% (v/v) water–acetonitrile solution buffered at pH 7.4 with 10 mM HEPES; (1) = Zn_2L–MTB ensemble + PPi, (2) = (1) + AcO^-, (3) = (1) + AMP, (4) = (1) + ADP, (5) = (1) + ATP, (6) = (1) + Br^-, (7) = (1) + Cl^-, (8) = (1) + F^-, (9) = (1) + I^-, (10) = (1) + BzO^-, (11) = (1) + CN^-, (12) = (1) + CO_3^{2-}, (13) = (1) + $H_2PO_4^-$, (14) = (1) + HCO_3^{2-}, (15) = (1) + PO_4^{3-}, (16) = (1) + NO_3^-, (17) = (1) + OH^-, (18) = (1) + SCN^- and (19) = (1) + SO_4^{2-}.

As shown in Fig. 9, even in the presence of a large excess of other competitive anions, no obvious interference with the detection of PPi was observed. These results clearly indicated

that the Zn_2L–MTB ensemble was useful for selectively sensing PPi even under competition from other related anions, which would fulfill the purpose of real-time monitoring. In addition, the detection limit of the absorption changes calculated on the basis of $3\sigma/K$ was 0.3 μM (Fig. S20, ESI†).[22]

4. Conclusions

We demonstrated for the first time that the tripodal tetramine dinuclear Zn(II) complex Zn_2L could be used to discriminate PPi from other phosphate containing anions under the indicator displacement assay using MTB as the indicator. Based on DFT calculations and NMR data, the binding mode of PPi to Zn_2L was the 2 : 2 complex species. It was found that the MTB indicator possessed suitable binding affinities with Zn_2L compared to the previously reported PV indicator found in dinuclear Zn(II)–DPA systems resulting in the high discrimination between PPi and other phosphate containing anions. Therefore, the new Zn_2L–MTB ensemble system could be used to detect PPi selectively with the detection limit of 0.3 μM in 20% (v/v) water–acetonitrile solution buffered at pH 7.4 with HEPES.

Acknowledgements

This work was supported by the Thailand Research Fund (RSA5580031 and RTA5380003) and the Center for Innovation in Chemistry (PERCH-CIC), Commission on Higher Education, Ministry of Education are gratefully acknowledged. S.W. is a Ph.D. student supported by the Royal Golden Jubilee Program (PHD/0236/2552). P.S. is a student supported by the Science Achievement Scholarship of Thailand.

Notes and references

1 A. E. Hargrove, S. Nieto, T. Zhang, J. L. Sessler and E. V. Anslyn, *Chem. Rev.*, 2011, **111**, 6603.
2 (*a*) S. K. Kim, D. H. Lee, J.-I. Hong and J. Yoon, *Acc. Chem. Res.*, 2009, **42**, 23 and references there in; (*b*) D. J. Liu, G. M. Credo, X. Su, K. Wu, H. C. Lim, O. H. Elibol, R. Bashir and M. Varma, *Chem. Commun.*, 2011, **47**, 8310; (*c*) J. F. Zhang, M. Park, W. X. Ren, Y. Kim, S. J. Kim, J. H. Jung and J. S. Kim, *Chem. Commun.*, 2011, **47**, 3568; (*d*) G. Su, Z. Liu, Z. Xie, F. Qian, W. He and Z. Guo, *Dalton Trans.*, 2009, 7888; (*e*) C. R. Lohani, J.-M. Kim, S.-Y. Chung, J. Yoon and K.-H. Lee, *Analyst*, 2010, **135**, 2079; (*f*) P. Sokkalingam, D. S. Kim, H. Hwang, J. L. Sessler and C.-H. Lee, *Chem. Sci.*, 2012, **3**, 1819; (*g*) S. Yang, G. Feng and N. H. Williams, *Org. Biomol. Chem.*, 2012, **10**, 5606; (*h*) L. J. Liang, X. J. Zhao and C. Z. Huang, *Analyst*, 2012, **137**, 953.
3 (*a*) P. Nyrén, *Anal. Biochem.*, 1987, **167**, 235; (*b*) M. Ronaghi, S. Karamohamed, B. Pettersson, M. Uhlen and P. Nyren, *Anal. Biochem.*, 1996, **242**, 84; (*c*) T. Tabary and L. J. Ju, *Immunol. Methods*, 1992, **156**, 55.
4 (*a*) M. Doherty, C. Becher, M. Regan, A. Jones and J. Ledingham, *Ann. Rheum. Dis.*, 1996, **66**, 432; (*b*) A. E. Timms, Y. Zhang, R. G. Russell and M. A. Brown, *Rheumatology*, 2002, **41**, 275.
5 (*a*) S. L. Wiskur, H. Ait-Haddou, J. J. Lavigne and E. V. Anslyn, *Acc. Chem. Res.*, 2001, **34**, 963; (*b*) J. J. Lavigne and E. V. Anslyn, *Angew. Chem., Int. Ed.*, 1999, **38**, 3666; (*c*) B. T. Nguyen and E. V. Anslyn, *Coord. Chem. Rev.*, 2006, **250**, 3118.
6 (*a*) H. T. Ngo, X. Liu and K. A. Jolliffe, *Chem. Soc. Rev.*, 2012, **41**, 4928; (*b*) A. J. Surman, C. S. Bonnet, M. P. Lowe, G. D. Kenny, J. D. Bell, E. Tóth and R. Vilar, *Chem. – Eur. J.*, 2011, **17**, 223.
7 (*a*) K. M. K. Swamy, S. K. Kwon, H. N. Lee, S. Kumar, J. S. Kim and J. Yoon, *Tetrahedron Lett.*, 2007, **48**, 8683; (*b*) S. Y. Kim and J.-I. Hong, *Tetrahedron Lett.*, 2009, **50**, 1951; (*c*) R. G. Hanshaw, S. M. Hilkert, H. Jiang and B. D. Smith, *Tetrahedron Lett.*, 2004, **45**, 8721; (*d*) J. V. Carolan, S. J. Butler and K. A. Jolliffe, *J. Org. Chem.*, 2009, **74**, 2992; (*e*) H. H. Jang, S. Yi, M. H. Kim, N. H. Lee and M. S. Han, *Tetrahedron Lett.*, 2009, **50**, 624.
8 (*a*) L. Tang, Y. Li, H. Zhang, Z. Guo and J. Qian, *Tetrahedron Lett.*, 2009, **50**, 6844; (*b*) J. H. Lee, J. Park, M. S. Lah, J. Chin and J.-I. Hong, *Org. Lett.*, 2007, **9**, 3729; (*c*) B. P. Morgans, S. He and R. C. Smith, *Inorg. Chem.*, 2007, **46**, 9262; (*d*) J. Gao, T. Riis-Johannessen, R. Scopelliti, X. Qian and K. Severin, *Dalton Trans.*, 2010, **39**, 7114.
9 (*a*) K. K. Y. Yuen and K. A. Jolliffe, *Chem. Commun.*, 2013, **49**, 4824; (*b*) X. Liu, H. T. Ngo, Z. G. Stephen, S. J. Butler and K. A. Jolliffe, *Chem. Sci.*, 2013, **4**, 1680; (*c*) Z.-H. Chen, Y. Lu, Y. B. He and X.-H. Huang, *Sens. Actuators, B*, 2010, **149**, 407.
10 C. S. Burdette, W. Bu and J. S. Lippard, *J. Am. Chem. Soc.*, 2003, **125**, 1778.
11 S. Watchasit, A. Kaowliew, C. Suksai, T. Tuntulani, W. Ngeonate and C. Pakawatchai, *Tetrahedron Lett.*, 2010, **51**, 3398.
12 R. A. Binstead, B. Jung and A. D. Zuberbühler, *SPECFIT/32 Global analysis System, 3.0*, Spectrum Software Associates, Marlborough, MA, 2000.
13 C. Incarvito, B. Rhatigan, L. A. Rheingold, J. C. Qin, L. A. Gavrilova and B. Bosnich, *J. Chem. Soc., Dalton Trans.*, 2001, 3478.
14 (*a*) M. Benamor, K. Belhamel and M. T. Draa, *J. Pharm. Biomed. Anal.*, 2000, **23**, 1033; (*b*) J. Ghasemi and S. Seifi, *Talanta*, 2004, **63**, 751; (*c*) I. M. Steinberg, A. Lobnik and O. S. Wolfbeis, *Sens. Actuators, B*, 2003, **90**, 230.
15 H. H. Jang, S. Yi, M. H. Kim, S. Kim, N. H. Lee and M. S. Han, *Tetrahedron Lett.*, 2009, **50**, 6241.
16 O. F. Ikotun, N. Marino, P. E. Kruger, M. Julve and R. P. Doyle, *Coord. Chem. Rev.*, 2010, **254**, 890.
17 A. D. Becke, *J. Chem. Phys.*, 1993, **98**, 5648.
18 C. Lee, W. Yang and R. G. Parr, *Phys. Rev. B: Condens. Matter*, 1988, **37**, 785.

19 P. J. Hay and W. R. Wadt, *J. Chem. Phys.*, 1985, **82**, 270.
20 M. J. Frisch, *et al.*, *GAUSSIAN 09 (Revision D.01)*, Gaussian Inc., Wallingford, CT, 2014.
21 H. N. Lee, Z. Xu, S. K. Kim, K. M. K. Swamy, Y. Kim, S.-J. Kim and J. Yoo, *J. Am. Chem. Soc.*, 2007, **129**, 3828.
22 Detection limit is defined by $3\sigma/K$, where σ refers to the standard deviation of the blank solutions and K is the slope of the linear regression curve observed in Fig. S12 in the ESI.† See: M. Hu and G. Feng, *Chem. Commun.*, 2012, **48**, 6951.